Bulletin of Electrical Engineering and Informatics
Vol. 13, No. 2, April 2024, pp. 963∼972
ISSN: 2302-9285, DOI: 10.11591/eei.v13i2.5949

On the outage performance analysis of $\alpha - \kappa - \mu$ fading channels with non-orthogonal multiple access protocol

Si-Phu Le[1], Hong-Nhu Nguyen[2], Nguyen Thi Hau[2], Nguyen Thi Thu Hang[2], Miroslav Voznak[1]
[1]Faculty of Electrical Engineering and Computer Science, VSB-Technical University of Ostrava, Ostrava, Czech Republic
[2]Faculty of Electronics and Telecommunications, Saigon University (SGU), Ho Chi Minh City, Vietnam

Article Info

Article history:

Received Feb 7, 2023
Revised Sep 23, 2023
Accepted Oct 24, 2023

Keywords:

$\alpha - \kappa - \mu$ fading channels
Bit error rate
Imperfect success interference cancellation
Non-orthogonal multiple access
Outage probability

ABSTRACT

In this paper, we consider effective performance transmission under generalized $\alpha - \kappa - \mu$ the fading distribution. The source-user links are assumed to be non-orthogonal multiple access (NOMA) channels through a downlink power domain. Two users are selected to service in a situation with perfect channel state information (CSI) in accordance with the NOMA protocol. The closed-form expressions of outage probability (OP) and bit error rate (BER) are derived with the effect of power allocation coefficient, target rate, and channel fading parameters. In addition, we calculate numerical results to demonstrate the asymptotic expansion in the high signal-to-noise ratio (SNR) analysis. Finally, Monte Carlo simulations are provided to validate and assess the accuracy of the analytical framework proposed.

Corresponding Author:

Hong-Nhu Nguyen
Faculty of Electronics and Telecommunications, Saigon University (SGU)
273 An Duong Vuong Street, Ward 3, District 5, 70000, Ho Chi Minh City, Vietnam
Email: nhu.nh@sgu.edu.vn

1. INTRODUCTION

The degradation of signal quality in wireless networks, commonly referred to as fading channels, has the potential to significantly impact transmission performance. Wireless downlink channels are of significant importance in the design of wireless communication systems. Moreover, the presence of wireless fading channels, which are responsible for shadowing effects, holds significant importance in the communication between the transmitter and receiver. Additional significant phenomena may be taken into account in order to effectively depict the deteriorating environment. Signal variation can be characterized by several probability distributions, including Hoyt, Rayleigh, Rice, Nakagami-m, and Weibull distributions. These distributions account for factors such as the characteristics of the propagation medium, the power of the dominating signal components, and the power of the dispersed waves. The key to a more detailed description is to understand the assumptions coming from the previous distributions. The study conducted by Moualeu *et al.* [1] and Lei *et al.* [2] investigates the performance and physical layer security (PLS) of wireless systems in the presence of generalized $\alpha - \kappa - \mu$ and $\alpha - \eta - \mu$ fading channels. In a similar vein, wireless-powered cooperative networks (WPCNs) are utilized in scenarios including a malevolent eavesdropper, while also serving as a benevolent jamming entity. The researches in [3], [4] have conducted an analysis on the transmit channels $\alpha - \kappa - \mu$ and $\alpha - \eta - \mu$, considering arbitrary fading parameters. The objective of their study is to investigate the impact of these channels on the performance of wireless networks. The utilization of spectrum sensing in wireless sensor networks (WSNs) has been extensively studied, particularly in relation to the aggregated $\alpha - \eta - \mu$/gamma and $\alpha - \kappa - \mu$/gamma

fading channels [5], [6].

The phenomenon known as the internet of things (IoT) encompasses a multitude of interconnected devices engaged in communication, hence presenting the challenge of limited availability of radio frequency spectrum. Spectrum sensing is a fundamental operation within the realm of cognitive radio, with power detectors serving as the prevailing method employed for this purpose. The issue at hand has been addressed in many scholarly articles that have examined the performance of the energy detector (ED) in the context of the $\alpha - \eta - \mu$ fading channel [7]–[10]. In the cited works by [11]–[13], the authors examined the application of non-orthogonal multiple access (NOMA) in a scenario where multiple users were considered. Specifically, two users were chosen to be served using the NOMA principle, assuming complete channel state information. The fading channels studied in this study were $\eta - \mu$ and $\kappa - \mu$ channels. The outage probability (OP), bit error rate (BER), and ergodic capacity (EC) were computed in previous studies [14]–[17].

The utilization of NOMA techniques has garnered significant interest due to its potential to enhance the throughput of wireless networks. These approaches are particularly important in the realm of communication system control. Moreover, through an examination of the encoding and decoding procedures employed in existing NOMA studies, it is shown that the technique of success interference cancellation (SIC) is utilized for signal demodulation, representing a significant demodulation approach inside the NOMA framework. Wu *et al.* [18] conducted extensive simulations to evaluate the block-error-rate performance of the NOMA schemes. These simulations align with the theoretical analysis presented in the paper. In relation to the aforementioned study, the researchers also conducted an analysis on the attainable rate of NOMA system. Their findings indicate that the achievable rate of the NOMA system can surpass that of the orthogonal multiple access (OMA) scheme [19], [20]. The study conducted by [21] investigates the impact of fixed power allocation on fading Nakagami-m channels for affected users in the reference scenario. The metric known as quality of service (QoS) holds significant importance as a performance indicator inside cellular networks. The study conducted an examination of indoor NOMA systems that utilize intelligent reflecting surfaces (IRS) in the context of generalized fading channels, as reported in the research article by [22], [23]. Qiu *et al.* [24] introduced a novel NOMA system wherein all user signals are allocated to block-fading channels. This allocation is directly linked to the symbol error rate for receivers that decode a user's signal.

This research has utilized the cooperation approach of a NOMA protocol and SIC technique, drawing inspiration from the aforementioned studies. The objective is to enhance the OP performance and conduct a BER analysis for the wireless network under consideration. In order to achieve the aforementioned objectives, our study aims to develop a wireless network architecture that operates in the presence of generalized $\alpha - \kappa - \mu$ fading channels. This design will incorporate considerations such as target rate and the distance between the ground and the base station. The present study aims to elucidate the contribution of this paper in the following manner:

- The closed-form equations for the OP and BER for users are derived.
- The asymptotic analysis of the OP in the high signal-to-noise ratio (SNR) regime is examined.
- The performance of the system and the BER are validated using numerical simulations in generalized $\alpha - \kappa - \mu$ fading channels with NOMA protocol.

The subsequent sections of the paper are structured in the following manner: section 2 provides an overview of the system model for NOMA in the downlink scenario, specifically focusing on generalized channels. Section 3 provides a performance study utilizing the suggested system model and the algorithms under analysis. Section 4 asymptotic analysis of the system under high SNR conditions, analysis of throughput and BER. Section 5 validation of numerical findings using Monte Carlo simulation. Section 6 provides a summary of the findings and outcomes obtained in this paper.

2. SYSTEM MODEL

Consider the concept of a downlink. The NOMA transmission method is employed in Figure 1 in scenarios when a solitary base station (BS) serves two active users simultaneously. In this system, the BS transmits signals for both users concurrently, utilizing the same frequency and time slots. In the context of a downlink scenario, the transfer signals originating from the near user (D_n) and distant user (D_f) will be assigned a designated power allocation and subsequently combined to form a unified stream for propagation.

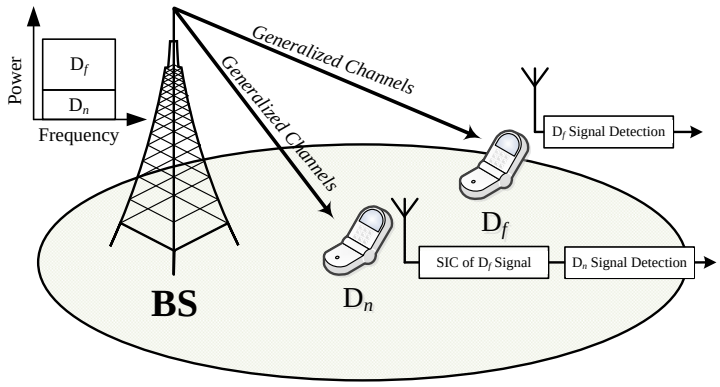

Figure 1. System model of NOMA for downlink with generalized $\alpha - \kappa - \mu$ fading

The received signal of each user's terminal can be represented by a mathematical model:

$$\bar{y}_{D_i} = h_{D_i}\left(\sqrt{\frac{a_1 P_S}{d_i^\beta}}\bar{x}_1 + \sqrt{\frac{a_2 P_S}{d_i^\beta}}\bar{x}_2\right) + \bar{n}_i \quad , i \in (f, n) \tag{1}$$

where h_{D_i} denotes the $\alpha - \kappa - \mu$ fading channel between BS and two users, $i \in (f, n)$ means the parameter belongs to the far user and near the user, P_S is the transmit power at the BS, β refers to the path-loss factor, while d_i shows the distance between the user and the BS, $\bar{x}_1$ and $\bar{x}_2$ are the superimposed signal vector satisfying the total power constraint $\mathbb{E}\left\{\bar{x}_1^2\right\} = \mathbb{E}\left\{\bar{x}_2^2\right\} = 1$. The relevant power allocation coefficients are a_1 and a_2. We assume that $a_1 < a_2$ with $a_1 + a_2 = 1$ to ensure better user fairness and $\bar{n}_i$ denotes the additive white Gaussian noise (AWGN) with $\bar{n}_i \sim CN\left(0, N_0\right)$.

Based on the above, we can obtain the Euclidean distance from BS to D_n and BS to D_f, respectively as [25]:

$$d_n = \sqrt{H^2 + d_{SD_n}^2} \tag{2a}$$

$$d_f = \sqrt{H^2 + d_{SD_f}^2} \tag{2b}$$

where d_{SD_n} is the distance between the ground and near user, d_{SD_f} is the distance between the ground and far user. The distance between the ground and the height of BS is denoted by H.

When D_n first notices that D_f has a higher transmit power and less inference signal, it can activate the SIC. Then, using the superposed signal, the signal of D_f may be found. The received signal-to-interference-plus-noise ratio (SINR) at D_n is therefore given by:

$$\bar{\gamma}_{D_n}^{x_2} = \frac{P_S a_2 |h_{D_n}|^2}{P_S a_1 |h_{D_n}|^2 + d_n^\beta N_0} = \frac{\rho_S a_2 |h_{D_n}|^2}{\rho_S a_1 |h_{D_n}|^2 + d_n^\beta} \tag{3}$$

where $\rho_S = P_S / N_0$ is the transmit SNR.

Following SIC, D_n is given the received SINR to identify its own message $\bar{x}_1$ by:

$$\bar{\gamma}_{D_n}^{x_1} = \frac{\rho_S a_1 |h_{D_n}|^2}{\nu \rho_S a_2 |h_{D_n}|^2 + d_n^\beta} \tag{4}$$

where ν, $0 \leq \nu \leq 1$ represents the efficiency of SIC for $\bar{x_2}$ at the D_n. The cases $\nu = 0$ and $\nu = 1$ correspond to perfect SIC and imperfect SIC, respectively.

In contrast, D_f decodes its desired signal $\bar{x_2}$ by considering $\bar{x_1}$ as interference. Thus, the SINR at D_f is:

$$\bar{\gamma}_{D_f}^{x_2} = \frac{\rho_S a_2 \left|h_{D_f}\right|^2}{\rho_S a_1 \left|h_{D_f}\right|^2 + d_f^\beta} \tag{5}$$

3. PERFORMANCE ANALYSIS

This portion of the study summarizes how well each user performed throughout outages in terms of outage likelihood. The chance that the message cannot be decoded at the intended receiver is quantified by such an outage indicator in more detail. Assume that all receivers are capable of receiving specific channel values.

3.1. The $\alpha-\kappa-\mu$ fading distribution

The small-scale fluctuation of the fading channel with a line-of-sight (LoS) component can be shown by the general distribution known as the $\alpha-\kappa-\mu$. As special examples, it contains Rayleigh, Nakagami-m, Rice, Weibull, one-sided Gaussian, and the fading distributions channel. The instantaneous SNR's PDF may be expressed as [1] (3):

$$f_{\gamma_i}(x)=\frac{\alpha}{e^{\kappa\mu}}\sum_{l=0}^{\infty}\frac{\mu^{\mu+2l}\kappa^l(1+\kappa)^{\mu+l}}{l!\Gamma(\mu+l)}x^{\alpha(\mu+l)-1}e^{-\mu(1+\kappa)x^{\alpha}} \tag{6}$$

where $\gamma_i \triangleq |h_{D_i}|^2, i\in\{f,n\}$, α, κ and μ is so-called non-negative real shape parameters. $\Gamma(.)$ is the Gamma function [26] (8.310.1).

Then, the cumulative distribution function (CDF) of $\alpha-\kappa-\mu$ distribution of SNR is given as [1] (7):

$$F_{\gamma_i}(x)=\sum_{l=0}^{\infty}\frac{\mu^l\kappa^l e^{-\kappa\mu}}{l!\Gamma(\mu+l)}\Upsilon(\mu+l,\mu(1+\kappa)x^{\alpha}) \tag{7}$$

where $\Upsilon(.,.)$ represents the lower incomplete Gamma function [26] (8.350.1).

We make use of the equalities [27] (2.6) as $\Upsilon(a,x)=G_{1,2}^{1,1}\left(x\middle|\begin{matrix}1\\a,0\end{matrix}\right)$, in which $G_{p,q}^{m,n}[.]$ is the Meijer G-function. After a few transformation steps (7) is rewritten as (8):

$$F_{\gamma_i}(x)=\sum_{l=0}^{\infty}\frac{\mu^l\kappa^l e^{-\kappa\mu}}{l!\Gamma(\mu+l)}G_{1,2}^{1,1}\left(\mu(1+\kappa)x^{\alpha}\middle|\begin{matrix}1\\\mu+l,0\end{matrix}\right) \tag{8}$$

3.2. Outage probability of D_n

According to NOMA protocol, the complementary events of outage at D_n can be explained as: D_n can detect $\bar{x}_2$ as well as its own message $\bar{x}_1$. From the description, the outage probability of D_n with imperfect SIC is expressed as (9):

$$\begin{aligned}OP_{D_n}&=1-\Pr\left(\bar{\gamma}_{D_n}^{x_2}>\gamma_{th2},\bar{\gamma}_{D_n}^{x_1}>\gamma_{th1}\right)=1-\Pr\left(|h_{D_n}|^2>\vartheta_2,|h_{D_n}|^2>\vartheta_1\right)\\&=1-\Pr\left(|h_{D_n}|^2>\vartheta_{\max}\right)=F_{|h_{D_n}|^2}(\vartheta_{\max})\end{aligned} \tag{9}$$

where the threshold SNRs are $\gamma_{th1}=2^{2R_1}-1$ with R_1 being the target rate at D_n to detect $\bar{x}_1$, $\gamma_{th2}=2^{2R_2}-1$ with R_2 being the target rate at D_n to detect $\bar{x}_2$, $\vartheta_1=\frac{\gamma_{th1}d_n^{\beta}}{\rho_S(a_1-\gamma_{th1}\nu a_2)}$, $\vartheta_2=\frac{\gamma_{th2}d_f^{\beta}}{\rho_S(a_2-\gamma_{th2}a_1)}$ and $\vartheta_{\max}=\max(\vartheta_1,\vartheta_2)$.

With the help of CDF in (7), the closed-form expression for the outage probability of D_n with imperfect SIC is given by:

$$OP_{D_n}=\sum_{l=0}^{\infty}\frac{\mu^l\kappa^l e^{-\kappa\mu}}{l!\Gamma(\mu+l)}G_{1,2}^{1,1}\left(\mu(1+\kappa)\vartheta_{\max}^{\alpha}\middle|\begin{matrix}1\\\mu+l,0\end{matrix}\right) \tag{10}$$

3.3. Outage probability of D_f

Similar to this, the likelihood that $\bar{x}_2$ cannot be effectively received by D_f (sometimes referred to as the OP of D_f) is as (11):

$$OP_{D_f}=1-\Pr\left(\bar{\gamma}_{D_f}^{x_2}>\gamma_{th2}\right)\qquad=1-\Pr\left(|h_{D_f}|^2>\frac{\gamma_{th2}d_f^{\beta}}{\rho_S(a_2-\gamma_{th2}a_1)}\right)=F_{|h_{D_f}|^2}(\vartheta_2) \tag{11}$$

Similar to how OP_{D_f} may be solved to produce OP_{D_n}. So, the considered system OP_{D_f} is defined as (12):

$$OP_{D_f}=\sum_{l=0}^{\infty}\frac{\mu^l\kappa^l e^{-\kappa\mu}}{l!\Gamma(\mu+l)}G_{1,2}^{1,1}\left(\mu(1+\kappa)\vartheta_2^{\alpha_i}\middle|\begin{matrix}1\\\mu+l,0\end{matrix}\right) \tag{12}$$

4. ASYMPTOTIC ANALYSIS AT HIGH SNR, ANALYSIS OF THROUGHPUT, AND BIT ERROR RATE

Even though we have obtained the closed-form OP expression of the system under consideration, it is challenging to evaluate the system's variety and coding gain directly. So, we consider the OP's asymptotic behavior in the high SNR zone. Based on (7), the moment as $\rho_S \to \infty$, one may use [1] (15) to estimate the CDF of $F_{\gamma_i}(x)$ as (13):

$$F_{\gamma_i}^{\infty}(x) \approx \frac{\mu^{\mu-1}(1+\kappa)^{\mu} x^{\alpha\mu}}{\Gamma(\mu)\, e^{\kappa\mu}} \tag{13}$$

By making a substitution (13) into (11) and (9) we have the asymptotic OP behavior of D_n and D_f are given by:

$$OP_{D_n}^{\infty} = F_{|h_{D_n}|^2}^{\infty}(\vartheta_{\max}) = \frac{\mu^{\mu-1}(1+\kappa)^{\mu}\vartheta_{\max}^{\alpha\mu}}{\Gamma(\mu)\, e^{\kappa\mu}} \tag{14a}$$

$$OP_{D_f}^{\infty} = F_{|h_{D_f}|^2}^{\infty}(\vartheta_2) = \frac{\mu^{\mu-1}(1+\kappa)^{\mu}\vartheta_2^{\alpha\mu}}{\Gamma(\mu)\, e^{\kappa\mu}} \tag{14b}$$

In a delay-limited transmission mode, each user's system throughput may be assessed by its OP. A two-user NOMA system's associated outage throughput is therefore stated as (15a) and (15b):

$$\tau_{D_n} = (1 - OP_{D_n})\, R_1 \tag{15a}$$

$$\tau_{D_f} = \left(1 - OP_{D_f}\right) R_2 \tag{15b}$$

Additionally, we substitute (10) and (12) into (15a) and (15b), respectively. So, we obtain the throughput of all legitimate users.

The following is the BER closed-form expression of the near user (D_n) [28] (20):

$$P_{D_n}^{BER} = \mathbb{E}\left\{Q\left(\sqrt{v\bar{\gamma}_{D_n}^{x_1}}\right)\right\} = \frac{\sqrt{v}}{2\sqrt{2\pi}} \int_0^{\infty} \frac{e^{-\frac{v}{2}x}}{\sqrt{x}} F_{\bar{\gamma}_{D_n}^{x_1}}(x)\, dx \tag{16}$$

where $Q(\cdot)$ is the Gaussian error function, and v denotes the modulation method, with $v = 1$ implies binary phase-shift keying (BPSK) modulation and $v = 2$ means quadature phase shift keying (QPSK) modulation.

Next, from (9) we let $t = \frac{2\nu a_2}{a_1}x - 1 \to \frac{a_1(t+1)}{2\nu a_2} = x \to \frac{a_1}{2\nu a_2}dt = dx$ and with the help of Gaussian-Chebyshev quadrature [29] (25.4.38). The closed-form approximation of $P_{D_n}^{BER}$ can be given as (17):

$$\begin{aligned} P_{D_n}^{BER} &= \frac{\sqrt{v}}{2\sqrt{2\pi}} \sum_{l=0}^{\infty} \frac{\mu^l \kappa^l e^{-\kappa\mu}}{l!\Gamma(\mu+l)} \int_0^{\frac{a_1}{\nu a_2}} \frac{e^{-\frac{v}{2}x}}{\sqrt{x}} G_{1,2}^{1,1}\left(\mu(1+\kappa)\left[\frac{x d_n^{\beta}}{\rho_S(a_1 - x\nu a_2)}\right]^{\alpha} \middle| \begin{matrix} 1 \\ \mu+l, 0 \end{matrix}\right) dx \\ &= \frac{a_1\sqrt{v}}{4\nu a_2\sqrt{2\pi}} \sum_{l=0}^{\infty} \frac{\mu^l \kappa^l e^{-\kappa\mu}}{l!\Gamma(\mu+l)} \int_{-1}^{1} \frac{e^{-\frac{v}{2}\mathcal{G}(t)}}{\sqrt{\mathcal{G}(t)}} G_{1,2}^{1,1}\left(\mu(1+\kappa)\left[\frac{\mathcal{G}(t)\, d_n^{\beta}}{\rho_S(a_1 - \mathcal{G}(t)\nu a_2)}\right]^{\alpha} \middle| \begin{matrix} 1 \\ \mu+l, 0 \end{matrix}\right) dt \\ &\approx \frac{a_1\pi\sqrt{v}}{4Q\nu a_2\sqrt{2\pi}} \sum_{l=0}^{\infty}\sum_{q=1}^{Q} \frac{\mu^l \kappa^l e^{-\kappa\mu - \frac{v}{2}\mathcal{G}(\phi_q)}\sqrt{1-\phi_q^2}}{l!\Gamma(\mu+l)\sqrt{\mathcal{G}(\phi_q)}} G_{1,2}^{1,1}\left(\mu(1+\kappa)\left[\frac{\mathcal{G}(\phi_q)\, d_n^{\beta}}{\rho_S(a_1 - \mathcal{G}(\phi_q)\nu a_2)}\right]^{\alpha} \middle| \begin{matrix} 1 \\ \mu+l, 0 \end{matrix}\right) \end{aligned} \tag{17}$$

where $\mathcal{G}(t) = \frac{a_1(t+1)}{2\nu a_2}$ and $\phi_q = \cos\left(\frac{2q-1}{2Q}\pi\right)$.

Similarly, by solving $P_{D_n}^{BER}$ and after few steps, the closed-form approximation of the of $P_{D_f}^{BER}$ can be obtained as (18):

$$P_{D_f}^{BER} \approx \frac{a_2\pi\sqrt{v}}{4Qa_1\sqrt{2\pi}} \sum_{l=0}^{\infty}\sum_{q=1}^{Q} \frac{\mu^l \kappa^l e^{-\kappa\mu - \frac{v}{2}\Lambda(\phi_q)}\sqrt{1-\phi_q^2}}{l!\Gamma(\mu+l)\sqrt{\Lambda(\phi_q)}} G_{1,2}^{1,1}\left(\mu(1+\kappa)\left[\frac{\Lambda(\phi_q)\, d_f^{\beta}}{\rho_S(a_2 - \Lambda(\phi_q)\, a_1)}\right]^{\alpha} \middle| \begin{matrix} 1 \\ \mu+l, 0 \end{matrix}\right) \tag{18}$$

where $\Lambda(t) = \frac{a_2(t+1)}{2a_1}$ and $\phi_q = \cos\left(\frac{2q-1}{2Q}\pi\right)$.

5. NUMERICAL RESULTS

In this paper, we illustrate outage performance by numerically simulating different theoretical findings from several metrics. The primary system parameters are set at $a_1 = 0.1$, $a_2 = 0.9$, $R_1 = R_2 = 1$, $H = 50$ m, $d_{SD_n} = 10$ m, $d_{SD_f} = 50$ m, $\beta = 2$, and $\nu = 0.01$. These distributions may be obtained from the $\alpha - \kappa - \mu$ fading distributions, as shown in Table 1. In addition, the Gauss-Chebyshev parameter is selected as $Q = 30$ to yield a close approximation.

Table 1. Distribution $\alpha - \kappa - \mu$ and the other fading distributions [3]

Channels	Parameters of the $\bar{\alpha} - \bar{\kappa} - \bar{\mu}$ distribution
Rayleigh	$\bar{\alpha} = 2, \bar{\kappa} = 0, \bar{\mu} = 1$
Nakagami-m	$\bar{\alpha} = 2, \bar{\kappa} = 0, \bar{\mu} = m$
Rician with parameter K	$\bar{\alpha} = 2, \bar{\kappa} = K, \bar{\mu} = 1$
$\kappa - \mu$	$\bar{\alpha} = 2, \bar{\kappa} = \kappa, \bar{\mu} = \mu$
$\alpha - \mu$	$\bar{\alpha} = \alpha, \bar{\kappa} = 0, \bar{\mu} = \mu$
Weibull	$\bar{\alpha} = \alpha, \bar{\kappa} = 0, \bar{\mu} = 1$

In Figure 2, the curves depicting the traditional fading channels are presented. Based on the visual representation, it is apparent that there is a significant enhancement in the performance of Nakagami-m. The impact of augmenting the SNR results in a discernible enhancement in the overall performance of the system. This performance is analogous to the one depicted in Figure 3. This example demonstrates the variation in outage likelihood across different levels of ipSIC (ν). When comparing the performance of OP_{D_n} using NOMA and OMA techniques, this figure demonstrates a more significant improvement.

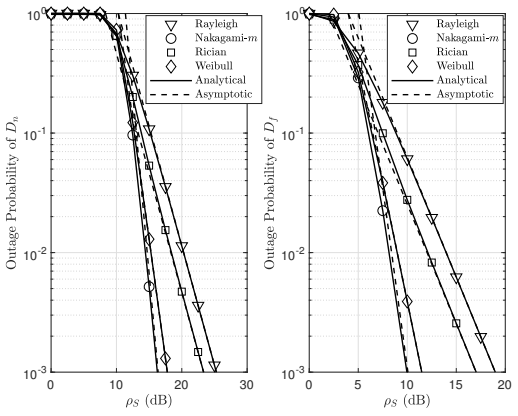

Figure 2. Comparison of classic channel the outage probability versus ρ_S

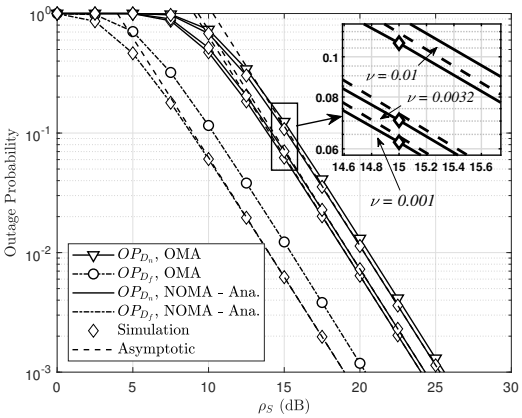

Figure 3. Outage probability versus ρ_S for different ν, with $R_1 = R_2 = 1$. $\alpha = 2$, $\kappa = 0$, and $\mu = 1$

The optimal outage performance may be observed by modifying the power allocation factor a_2, as depicted in Figure 4. It can be understood that in (3)-(5), the SINRs are influenced by the power allocation variables. Consequently, the behavior of outages is determined by these power allocation factors. The observed variation in performance between the two users can be attributed to the power constraint. Regrettably, the task of establishing the optimal outage probability for a remote user is likely to present significant challenges. A higher SNR at the source, denoted as $\rho_S = 10$ dB, is commonly seen as a more favorable scenario.

The Figure 5 illustrates the throughput performance for both nearby users and distant users. The proposed methods, namely, provide increased data transfer rates under conditions of high SNR. However, due to the fact that the value of ρ_S exceeds 30 dB, the throughput attains its maximum limit. The throughput is determined exclusively by the intended goal rates at high levels, which is the underlying cause for the high value of ρ_S.

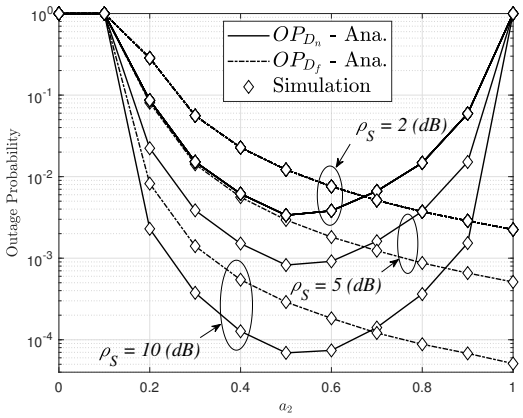

Figure 4. OP versus power allocation factor a_2, with $R_1 = R_2 = 0.1$, $\alpha = 2$, $\kappa = 0$, and $\mu = 1$

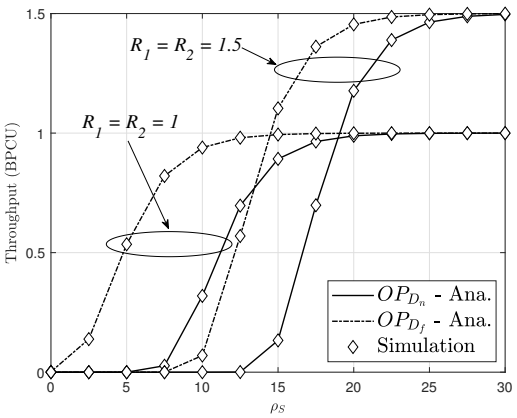

Figure 5. Throughput in delay-limited transmission mode versus ρ_S with different values of R_1 and R_2

Figure 6 depicts the OP vs distance between BS-d_{SD_n} (Figure 6 (a)) and BS-d_{SD_f} (Figure 6(b)) at various heights. The OP of the two users is significantly different at a wider distance, however the outage performance of the two users is high when they are closer to the BS. Furthermore, we estimate that the height of the BS has a significant impact on the outage likelihood failure when it is too high, namely $H = 50$ (m) and $H = 75$ (m).

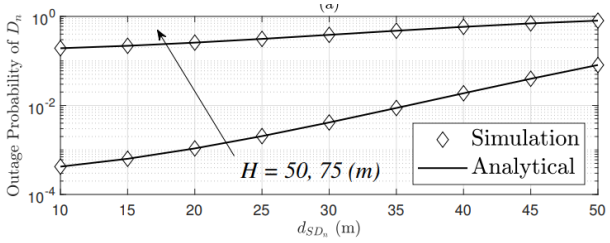

(a)

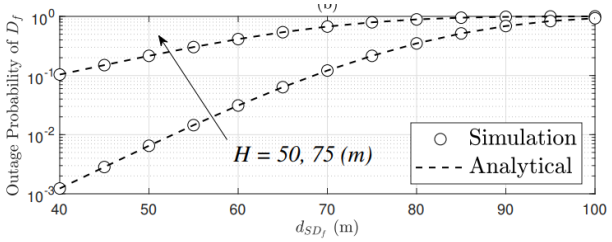

(b)

Figure 6. OP versus; (a) d_n at D_n and (b) d_f at D_f, with $R_1 = 1$, $R_2 = 2$, $\beta = 3$, $\alpha = 2$, $\kappa = 0$, $\mu = 3$, and $\rho_S = 74$ (dB)

Figure 7 depicts the BER of the NOMA communication system under consideration versus the average SNR for BPSK ($\upsilon = 1$) and QBSK ($\upsilon = 2$) modulations. In Figure 7, $\nu = 0.01$, $\alpha = 2$, $\kappa = 0$, and $\mu = 1$ is used. It is clear that in the low SNR zone, the BERs of the near and far users differ only little. However, in the high SNR zone, the BER of the distant user degrades significantly more than that of the close user. When BER = 10^2, the gains in the average BER of the near user relative to the distant user are approximately 10 (dB) for BPSK and 20 (dB) for QPSK, respectively. The BER of a distant user, on the other hand, approaches saturation at $\rho_S = 25$ (dB), while the BER of near user continuously decreases.

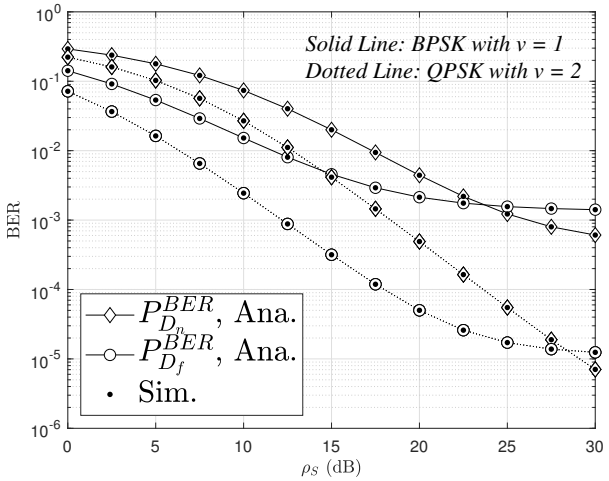

Figure 7. The BER performance varies with transmitting power, with $\alpha = 2$, $\kappa = 0$ and $\mu = 1$

6. CONCLUSION

This study included an analysis of the performance of NOMA in downlink communication networks. The closed-form expression of OP and throughput are calculated, in which the BER of the NOMA communication system is considered versus the average SNR to evaluate the transmission efficiency of the system. Monte Carlo simulations used to validate analytical findings. In this study, we present numerical findings pertaining to diverse performance metrics across many parameters, including power allocation factor, target rate, and the influence of generalized $\alpha - \kappa - \mu$ fading channels. It has been determined that the downlink NOMA system offers equitable treatment to users within the proposed system paradigm. Our theoretical analyses are constructed to analyze the performance of NOMA downlink systems over generalized fading channels. We want to examine the impact of different parameters on the system's performance. In the future, the efficacy of the NOMA system is anticipated to be enhanced by the integration of transmission, energy harvesting, and secrecy analysis.

ACKNOWLEDGEMENT

The authors would like to thank the anonymous reviewers for their helpful comments and suggestions. This work is a part of the basic science research program CSB2022-50 funded by Saigon University. The research leading to these results was supported by the Czech Ministry of Education, Youth and Sports under project reg. no. SP2021/25 and also partially under the e-INFRA CZ project ID:90140.

REFERENCES

[1] J. M. Moualeu, D. B. da Costa, W. Hamouda, U. S. Dias and R. A. A. de Souza, "Physical Layer Security Over $\alpha - \kappa - \mu$ and $\alpha - \eta - \mu$ Fading Channels," in *IEEE Transactions on Vehicular Technology*, vol. 68, no. 1, pp. 1025-1029, Jan. 2019, doi: 10.1109/TVT.2018.2884832.

[2] H. Lei *et al.*, "Performance Analysis of Physical Layer Security Over Generalized-K Fading Channels Using a Mixture Gamma Distribution," in *IEEE Communications Letters*, vol. 20, no. 2, pp. 408-411, Feb. 2016, doi: 10.1109/LCOMM.2015.2504580.

[3] G. Fraidenraich and M. D. Yacoub, "The $\alpha - \eta - \mu$ and $\alpha - \kappa - \mu$ Fading Distributions," in *2006 IEEE Ninth International Symposium on Spread Spectrum Techniques and Applications*, 2006, pp. 16-20, doi: 10.1109/ISSSTA.2006.311725.

[4] S. Kumar, M. Kaur, N. K. Singh, K. Singh, and P. S. Chauhan, "Energy detection based spectrum sensing for gamma shadowed $\alpha - \eta - \mu$ and $\alpha - \kappa - \mu$ fading channels," in *AEU-International Journal of Electronics and Communications*, vol. 1, no. 93, pp. 26-31, Sep. 2018, doi: 10.1016/j.aeue.2018.05.031.

[5] V. D. Phan, T. L. Nguyen, T. T. Phu, and V. V. Nguyen, "Reliability-Security in Wireless-Powered Cooperative Network with Friendly Jammer," in *Advances in Electrical and Electronic Engineering*, vol. 20, no. 4, pp. 584-591, Feb. 2023, doi: 10.15598/aeee.v20i4.4511.

[6] P. S. Chauhan, P. Negi, and S. K. Soni, "A unified approach to modeling of probability of detection over $\alpha - \mu/IG$, $k - \mu/IG$, and $\eta - \mu/IG$ composite fading channels with application to cooperative system," in *AEU-International Journal of Electronics and Communications*, vol. 87, pp. 33-42, Apr 2018, doi: 10.1016/j.aeue.2018.01.035.

[7] T. R. Rasethuntsa and S. Kumar, "An integrated performance evaluation of ED-based spectrum sensing over $\alpha - \kappa - \mu$ and

$\alpha - \kappa - \mu$ - Extreme fading channels," in *Transactions on Emerging Telecommunications Technologies*, vol. 30, no. 5, May 2019, doi: 10.1002/ett.3569.

[8] S. Kumar, "Performance of ED based spectrum sensing over $\alpha - \eta - \mu$ fading channel," in *Wireless Personal Communications 100*, pp. 1845-57, Jun. 2018, doi: 10.1007/s11277-018-5677-6.

[9] A. Bagheri, P. C. Sofotasios, T. A. Tsiftsis, A. Shahzadi, and M. Valkama, "AUC study of energy detection based spectrum sensing over $\eta - \mu$ and $\alpha - \mu$ fading channels," in *2015 IEEE International Conference on Communications (ICC)*, 2015, pp. 1410-1415, doi: 10.1109/ICC.2015.7248521.

[10] S. K. Yoo *et al.*, "The $\kappa - \mu$ / Inverse Gamma and $\eta - \mu$ / Inverse Gamma Composite Fading Models: Fundamental Statistics and Empirical Validation," in *IEEE Transactions on Communications*, vol. 69, no. 8, pp. 5514-5530, Aug. 2021, doi: 10.1109/TCOMM.2017.2780110.

[11] C.-B. Le, H.-N. Nguyen, H.-H. Nguyen, T.-H. Nguyen, and N.-D. Nguyen, "Outage performance analysis of NOMA over log-normal fading distribution in presence of CSI and SIC imperfections," in *Bulletin of Electrical Engineering and Informatics*, vol. 11, no. 3, pp. 1428-1437, Jun 2022, doi: 10.11591/eei.v11i3.3395.

[12] P. Sharma, A. Kumar, and M. Bansal, "Performance analysis for user selection-based downlink non-orthogonal multiple access system over generalized fading channels," in *Transactions on Emerging Telecommunications Technologies*, vol. 32, no. 11, p. e4347, Nov. 2021, doi: 10.1002/ett.4347.

[13] C.-B Le, H.-N Nguyen, N.-L Nguyen, M. Voznak, and N.-D Nguyen, "Considering the $\kappa - \mu$ fading channels adopted in multiple antennas downlink non-orthogonal multiple access," in *Bulletin of Electrical Engineering and Informatics*, vol. 11, no. 1, pp. 336-345, Feb 2022, doi: 10.11591/eei.v11i1.3453.

[14] A. Alqahtani, E. Alsusa, A. Al-Dweik, and M. Al-Jarrah, "Performance Analysis for Downlink NOMA Over $\alpha - \mu$ Generalized Fading Channels," in *IEEE Transactions on Vehicular Technology*, vol. 70, no. 7, pp. 6814-6825, Jul. 2021, doi: 10.1109/TVT.2021.3082917.

[15] B. M. ElHalawany, F. Jameel, D. B. da Costa, U. S. Dias, and K. Wu, "Performance Analysis of Downlink NOMA Systems Over $\kappa - \mu$ Shadowed Fading Channels," in *IEEE Transactions on Vehicular Technology*, vol. 69, no. 1, pp. 1046-1050, Jan. 2020, doi: 10.1109/TVT.2019.2953109.

[16] L. Bariah, S. Muhaidat, and A. Al-Dweik, "Error Probability Analysis of Non-Orthogonal Multiple Access Over Nakagami-m Fading Channels," in *IEEE Transactions on Communications*, vol. 67, no. 2, pp. 1586-1599, Feb. 2019, doi: 10.1109/TCOMM.2018.2876867.

[17] K. Aslan and T. Gucluoglu, "Performance analysis of downlink-NOMA over generalized-k fading channels," in *Physical Communication*, vol. 48, p. 101414, Oct. 2021, doi: 10.1016/j.phycom.2021.101414.

[18] Z. Wu, K. Lu, C. Jiang, and X. Shao, "Comprehensive Study and Comparison on 5G NOMA Schemes," in *IEEE Access*, vol. 6, pp. 18511-18519, 2018, doi: 10.1109/ACCESS.2018.2817221.

[19] M. Jain, S. Soni, N. Sharma, and D. Rawal, "Performance analysis at far and near user in NOMA based system in presence of SIC error," in *AEU-International Journal of Electronics and Communications*, vol. 114, p. 152993, Feb 2020, doi: 10.1016/j.aeue.2019.152993.

[20] H. Yahya, E. Alsusa, and A. Al-Dweik, "Exact BER Analysis of NOMA With Arbitrary Number of Users and Modulation Orders," in *IEEE Transactions on Communications*, vol. 69, no. 9, pp. 6330-6344, Sep. 2021, doi: 10.1109/TCOMM.2021.3088526.

[21] T. Hou, X. Sun, and Z. Song, "Outage Performance for Non-Orthogonal Multiple Access With Fixed Power Allocation Over Nakagami- m Fading Channels," in *IEEE Communications Letters*, vol. 22, no. 4, pp. 744-747, Apr. 2018, doi: 10.1109/LCOMM.2018.2799609.

[22] P. Sharma, A. Kumar, and M. Bansal, "Performance analysis of downlink NOMA over $\eta - \mu$ and $\kappa - \mu$ fading channels," in *IET Communications*, vol. 14, no. 3, pp. 522-531, Feb. 2020, doi: 10.1049/iet-com.2019.0413.

[23] A. Alqahtani and E. Alsusa, "On the Quality of Service and Experience in IRS-NOMA Over $\kappa - \mu$ Generalized Fading Channels," in *IEEE Open Journal of the Communications Society*, vol. 3, pp. 2272-2283, 2022, doi: 10.1109/OJCOMS.2022.3222177.

[24] M. Qiu, Y. -C. Huang, and J. Yuan, "Downlink Non-Orthogonal Multiple Access Without SIC for Block Fading Channels: An Algebraic Rotation Approach," in *IEEE Transactions on Wireless Communications*, vol. 18, no. 8, pp. 3903-3918, Aug. 2019, doi: 10.1109/TWC.2019.2919292.

[25] B. Zhao, C. Zhang, W. Yi, and Y. Liu, "Ergodic rate analysis of star-ris aided noma systems," *IEEE Communications Letters*, vol. 26, no. 10, pp. 2297-2301, Jul. 2022, doi: 10.1109/LCOMM.2022.3194363.

[26] I. S. Gradshteyn and I. M. Ryzhik, *Table of Integrals, Series and Products*, 6th ed. New York, NY, USA: Academic Press, 2000.

[27] A. M. Mathai, R. K. Saxena, and H. J. Haubold, *The H-function: theory and applications*. Springer Science & Business Media, 2009.

[28] C.-B. Le, D.-T. Do, Z. Zaharis, C. Mavromoustakis, G. Mastorakis, and E. Markakis, "System performance analysis in cognitive radio aided NOMA network: An application to vehicle-to-everything communications," *Wireless Personal Communications*, vol. 120, no. 3, pp. 1975-2000, 2021, doi: 10.1007/s11277-021-08273-x.

[29] M. Abramowitz and I. A. Stegun, *Handbook of Mathematical Functions with Formulas, Graphs, and Mathematical Tables*. New York, NY, USA: Dover, 1972.

BIOGRAPHIES OF AUTHORS

Si-Phu Le was born in Da Nang city, Vietnam, in 1985. He received a B.Sc. from Nha Trang University, Nha Trang, Vietnam in 2008 and an M.B.A. from Open University of Malaysia in 2013. He was lecturer in IT Department of Van Lang University from 2009 to 2020. He is currently working as Managing Director at ACEXIS JSC. His research interests include electronic design, digital signal processing, MIMO, NOMA, and intelligent reflecting surfaces. He is studying Ph.D. in Telecommunication from Technical University of Ostrava, Czech Republic in 2023. He can be contacted at email: phu.le.si.st@vsb.cz.

Hong-Nhu Nguyen received a B.Sc. in Electronics Engineering from Ho Chi Minh City University of Technology in 1998, M.Eng. in Electronics Engineering from the University of Transport and Communications (Vietnam) in 2012 and his Ph.D. degree in telecommunication from Technical University of Ostrava, Czech Republic in 2021. He is currently working as lecturer at Saigon University. His research interests include applied electronics, wireless communications, cognitive radio, NOMA, and energy harvesting. He can be contacted at email: nhu.nh@sgu.edu.vn.

Nguyen Thi Hau was born in Binh Dinh Province, Vietnam, in 1984. She received a B.Sc. in Electronics Telecommunications Engineering from Da Nang University of Technology (Vietnam) in 2007 and an M.Sc. in Electronics Engineering from Ho Chi Minh City University of Technology (Vietnam) in 2011. She is currently working as lecturer at Saigon University. Her research interests include applied electronics, wireless communications, cognitive radio, NOMA, and energy harvesting. She can be contacted at email: hau.nt@sgu.edu.vn.

Nguyen Thi Thu Hang was born in Ho Chi Minh City, Vietnam, in 1976. She received a B.Sc. from Ho Chi Minh City University of Technology, Ho Chi Minh, Vietnam in 1999 and an M.Sc. in Electronics Telecommunications Engineering from Ho Chi Minh City University of Technology, Vietnam in 2002. She is currently working as a lecturer at Saigon University. Her research interests include electronic design, digital signal processing, ASIC design, and wireless communications. She can be contacted at email: hangntt@sgu.edu.vn.

Miroslav Voznak (M'09-SM'16) received his Ph.D. in telecommunications in 2002 from the Faculty of Electrical Engineering and Computer Science at VSB–Technical University of Ostrava, and achieved habilitation in 2009. He was appointed Full Professor in Electronics and Communications Technologies in 2017. His research interests generally focus on ICT, especially on quality of service and experience, network security, wireless networks, and big data analytics. He has authored and co-authored over one hundred articles in SCI/SCIE journals. According to the Stanford University study released in 2020, he is one of the World's Top 2% of scientists in Networking and Telecommunications and Information and Communications Technologies. He served as a general chair of the 11th IFIP Wireless and Mobile Networking Conference in 2018 and the 24th IEEE/ACM International Symposium on Distributed Simulation and Real Time Applications in 2020. He participated in six projects funded by the EU in programs managed directly by European Commission. Currently, he is a principal investigator in the research project QUANTUM5 funded by NATO, which focuses on the application of quantum cryptography in 5G campus networks. He can be contacted at email: miroslav.voznak@vsb.cz.